Prostaglandin Pathway Gene Therapy for Sustained Reduction of Intraocular Pressure

Román A Barraza[1], Jay W McLaren[2] and Eric M Poeschla[1]

[1]Department of Molecular Medicine, Mayo Clinic College of Medicine, Rochester, Minnesota, USA; [2]Department of Ophthalmology, Mayo Clinic College of Medicine, Rochester, Minnesota, USA

Cyclooxygenase-2 (COX-2) is a rate-limiting enzyme in prostaglandin (PG) biosynthesis. In the eye, loss of COX-2 expression in aqueous humor–secreting cells has been associated with primary open-angle glaucoma (POAG). Reduction of intraocular pressure (IOP) is the main treatment goal in this disease. We used lentiviral vectors to stably express COX-2 and other PG biosynthesis and response transgenes in the ciliary body epithelium and trabecular meshwork (TM), the ocular suborgans that produce aqueous humor and regulate its outflow, respectively. We show that robust ectopic COX-2 expression and PG production require COX-2 complementary DNA (cDNA) sequence optimization. When COX-2 expression was coupled with a similarly optimized synthetic $PGF_{2\alpha}$ receptor transgene to enable downstream signaling, gene therapy produced substantial and sustained reductions in IOP in a large animal model, the domestic cat. This study provides the first gene therapy for correcting the main cause of glaucoma.

Received 24 July 2009; accepted 6 November 2009; published online 1 December 2009. doi:10.1038/mt.2009.278

INTRODUCTION

Primary open-angle glaucoma (POAG) afflicts 70 million people and ranks just behind macular degeneration in causing irreversible vision loss. Blindness results from death of retinal neurons (ganglion cells) that connect via long axons with visual nuclei in the brain. The major causal risk factor in this disease is chronically increased intraocular pressure (IOP), which in turn results from increased resistance to the outflow of aqueous humor from the eye.[1] Aqueous humor is secreted continuously into the posterior chamber by the surface, nonpigmented epithelium (NPE) of the ciliary body, circulates through the pupil to the anterior chamber (AC) and exits the eye into the venous system via the trabecular and uveoscleral outflow pathways located in the AC periphery (**Supplementary Figure S1**). Functioning as the necessarily acellular, *i.e.*, transparent, equivalent of blood, aqueous humor nourishes, oxygenates, and removes products of metabolism from the lens, iris, and posterior cornea. The circulation is substantial (2.5–2.8 µl/min), which leads to full-volume exchange every few hours.

Reducing IOP is the main treatment strategy in glaucoma. Daily use of agents such as cholinergic and adrenoreceptor agonists, β-blockers, carbonic anhydrase inhibitors, and prostaglandin (PG) analogues can reduce IOP, but the transience of the effects necessitates daily reapplication, treatment adherence is poor in this lifelong disease, and efficacy is often partial even with combined medical-surgical interventions.[2] $PGF_{2\alpha}$ analogues are thought to act by activating the FP receptor (FPR) in the aqueous outflow pathway.[3]

PG biosynthesis begins with conversion of arachidonic acid to PGH_2 by COX-1 or cyclooxygenase (COX-2). This reaction step is rate-limiting.[4] PGH_2 is then converted by specific synthases to the different main biologically active prostanoids ($PGF_{2\alpha}$, PGE_2, PGD_2, PGI_2, or TXA_2), which signal through specific receptors (**Figure 1a**). COX-2 is generally characterized as the inducible form of cyclooxygenase, vis-à-vis constitutively expressed COX-1, although this dichotomy is now recognized as simplistic because constitutive COX-2 expression is also evident in multiple tissues, such as brain, ocular ciliary epithelium, vascular endothelium, kidney, pancreas, gonads, stomach, and colon.[4–7] How and why a given tissue or cell type employs a constitutive versus inducible COX-2 expression pattern is not understood.

Further contravening the initial paradigm of COX-2 expression as a strictly reactive response to extracellular inflammatory stimuli, antagonism, or loss of constitutive COX-2 expression is now known to have pathogenic potential. For example, systemic inhibition of COX-2, *e.g.*, with rofecoxib (VIOXX) elevates the risk of myocardial infarction and stroke, probably by blocking vascular endothelial PGI_2 production.[5,8] In the eye, a striking complete loss of normally constitutive NPE COX-2 expression was recently demonstrated to occur in POAG.[6] This observation is intriguing because it is the NPE that secretes aqueous humor. Whether this phenomenon is a cause or a consequence of the disease remains to be established, but a distinction compatible with the former interpretation was that COX-2 loss was seen in POAG (the common form of glaucoma) and corticosteroid-induced glaucoma, but not in the much less common angle-closure or juvenile-onset forms, which are also characterized by chronic IOP elevation.[6] In addition, recently available IOP-reducing agents appear to upregulate expression of COX-2 and PGs, as well as various other molecules with potential to decrease resistance to aqueous outflow, such as matrix metalloproteinases.[9,10]

Correspondence: *Eric M Poeschla, Department of Molecular Medicine, Guggenheim 18, Mayo Clinic College of Medicine, 200 First Street SW, Rochester, Minnesota, USA. E-mail: emp@mayo.edu*

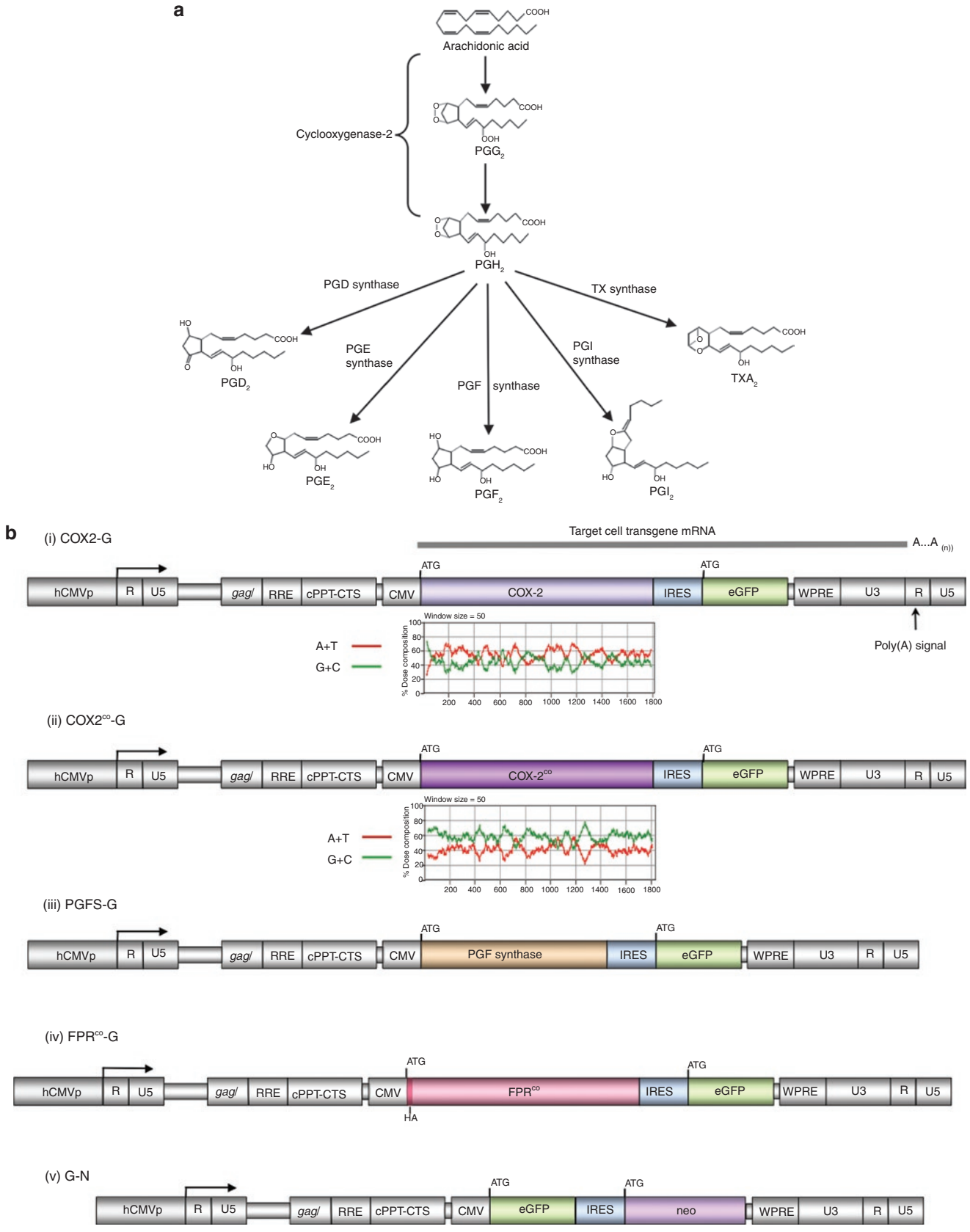

Glaucoma patients face substantial risk of progressive optic nerve damage because of the partial efficacies and long-term compliance burdens of current therapies.[11] Persistence with drug therapy at 1 year is consistently <50% (ref. 2). Permanent, single-step correction of IOP pathophysiology by gene therapy has attracted attention as a theoretically ideal alternative solution.[12] One factor in favor of this approach, particularly with integrating vectors, is the lifelong chronicity of the disease. In addition, the small amount of tissue involved and its confinement to a discrete AC region accessible by transcorneal injection[13] ameliorates problems of access, and in particular scale, that are frequently problematic for gene therapy. The relatively immunoprivileged environment of the eye also decreases the risk of prohibitive immune responses to viral vectors. Gene therapy directed at the retina to prevent ganglion cell death (neuroprotection) is also being pursued. For the IOP-reduction strategy, the trabecular meshwork (TM) is a prioritized target because it determines IOP by the resistance it generates to aqueous humor outflow. Although the potential promise of IOP-reducing gene therapy has been evident, the obstacle remains that therapeutic glaucoma transgenes have not been established. However, some marker gene transfer studies have established the feasibility of genetically modifying the critical tissues. Lentiviral vectors, which integrate permanently in postmitotic cells,[14] have attracted interest because eye tissues are terminally differentiated. Both feline immunodeficiency virus (FIV)–based lentiviral vectors and HIV-1-based lentiviral vectors have been shown to mediate sustained, high-level marker transgene expression in TM, whereas γ-retroviral (murine leukemia virus) vectors, which require target cells to be cycling, do not.[13,15–19]

Based on the known therapeutic efficacy of topical PG analogues and the loss of ocular COX-2 expression in POAG, we hypothesized here that *de novo* engineering of a constitutive COX-2-based PG biosynthesis and response pathway could be achieved *in vivo* with lentiviral vectors and that this could effectively reduce IOP if carried out within the AC of the eye.

RESULTS

AU-rich elements in the human COX-2 coding region diminish ectopic expression

An initial ambiguity was whether ectopic COX-2 expression alone would be sufficient to enable robust or constitutive PG synthesis. The need for an ectopically expressed downstream PG synthase was unclear, for example, as were potential roles of other unknown cellular proteins. To investigate this, we constructed a lentiviral transfer vector encoding the human COX-2 complementary DNA (cDNA) (vector COX2-G, **Figure 1b(i)**). Both COX-2 and GFP are expressed from a single internally promoted transgene mRNA to force coexpression of both genes and allow convenient titration and transgene monitoring. We used the coding region but excluded all of the 3′UTR because of its known RNA-destabilizing elements, *e.g.*, its 22 copies of a classical "AUUUA" element.[20–22] Nevertheless, we were unable to achieve substantial expression of COX-2 or PG production by either direct plasmid transfection or by lentiviral transduction with pCOX2-G. With the possible exception of Lu *et al.*, who selected a single cell clone having increased COX-2 expression from a stably transfected cell pool,[23] we were unable to find previous examples of robust ectopic human COX-2 expression from the cDNA. The issue is not addressed in prior studies of COX-2 expression or mRNA stability, which have focused either on regulation of the endogenous message or mapping the strongly destabilizing motifs in the 3′UTR by transferring this element to test genes such as firefly *luciferase*.

We therefore performed *in silico* analyses of the COX-2 mRNA coding region, which revealed a highly AU-rich base composition (**Supplementary Figure S2a**). This composition results in strongly nonoptimal human codon usage. The situation is also reminiscent of the marked AU-rich skewing of HIV-1 structural gene mRNAs (**Supplementary Figure S2b**), which are consequently rapidly degraded unless rescued by the HIV-1 Rev nuclear export pathway.[24] We therefore proceeded to optimize all of the human COX-2 cDNA codons, changing 382 of 1,815 nucleotides to create *COX-2^{co}* (**Supplementary Figure S2a**, bottom). When incorporated into a lentiviral vector [pCOX2^{co}-G, **Figure 1b(ii)**], the *COX-2^{co}* synthetic transgene produced a marked increase in both GFP and COX-2 expression, which was documented at both the protein and mRNA levels (**Figure 2a–c**). In these and other experiments, both proteins (COX-2 and GFP) were detected as single undergraded proteins of expected size (**Figure 2c**), COX-2 expression was always accompanied by GFP coexpression (**Figure 2c** and data not shown), and single mRNAs of expected size were found by quantitative reverse transcriptase–PCR and northern blotting, confirming the anticipated coordinated coexpression (**Figure 2b** and **Supplementary Figure S3**). $PGF_{2\alpha}$ production was also markedly increased by the synthetic COX-2 allele (**Figure 2d**). $PGF_{2\alpha}$ levels were >50-fold higher in supernatants of cells transduced with COX2^{co}-G vector compared to COX2-G vector, and >150-fold higher compared to G-N- or mock-transduced cultures.

Having determined that the steady-state mRNA levels are much higher with the COX2^{co}-G than with COX2-G transgene, we attempted to measure mRNA decay rates by northern analysis at

Figure 1 Prostaglandin biosynthesis pathways and lentiviral transfer vectors. (**a**) COX-2 catalyzes conversion of arachidonic acid to PGH_2 via PGG_2. This step is rate-limiting. PGH_2 is rapidly converted to a specific prostanoid by a specific synthase. The $PGF_{2\alpha}$ pathway is bolded. (**b**) Lentiviral transfer vectors. All are two-gene feline immunodeficiency virus vectors containing two complementary DNAs (cDNAs) in a single transcription unit, such that the upstream and downstream genes are translated from a single mRNA and were derived from later generation versions[42] of a prototype system.[48] Translation of the downstream gene initiates from the internal ribosome entry site (IRES), rather than the 5′ cap. The forced coexpression of GFP with each PG pathway gene simplifies and standardizes identification of transgene expression *in vivo* and titering of diverse vector stocks. The same internal promoter drives expression in all vectors (human CMV immediate-early gene promoter). Transfer vectors COX2-G, COX2^{co}-G, PGFS-G, and FPR^{co}-G contain a prostanoid pathway gene cDNA (wild-type human COX-2, codon-optimized human COX-2, human PGFS, and N-terminally HA-tagged, codon-optmized human FPR, respectively) and GFP. Control vector G-N encodes GFP and neoR. CMV, cytomegalovirus; cPPT-CTS, central polypurine tract-central termination sequence (DNA flap-generating elements);[49] eGFP, enhanced green fluorescent protein; *gag/*, truncated gag segment required for packaging signal;[50] hCMVp, CMV, human CMV immediate-early gene promoter; R, R repeat; RRE, Rev response element; U3, 3′ unique region; U5, 5′ unique region; WPRE, woodchuck hepatitis virus post-transcriptional regulatory element. Base composition plots are shown for human COX-2 and codon-optimized human COX-2 cDNA coding regions (see **Supplementary Figure S2** for detail).

serial time points after actinomycin D treatment, but, as shown in **Supplementary Figure S3**, not enough native cDNA-transcribed message could be detected at time zero to establish an accurate decay rate. Nevertheless, taken together, these results indicate that the difference occurs at the RNA level rather than at translation, and suggest that the COX-2 mRNA has sequence-dependent stability or trafficking vulnerability determined not only by the known 3′UTR elements,[20–22] but by the coding region as well, and this can be prevented by nucleotide sequence optimization. Moreover, these experiments probably underestimate the defect because it is likely diluted by the downstream expression-optimal segments in the vector transgene mRNAs (*e.g.*, *eGFP*, WPRE).

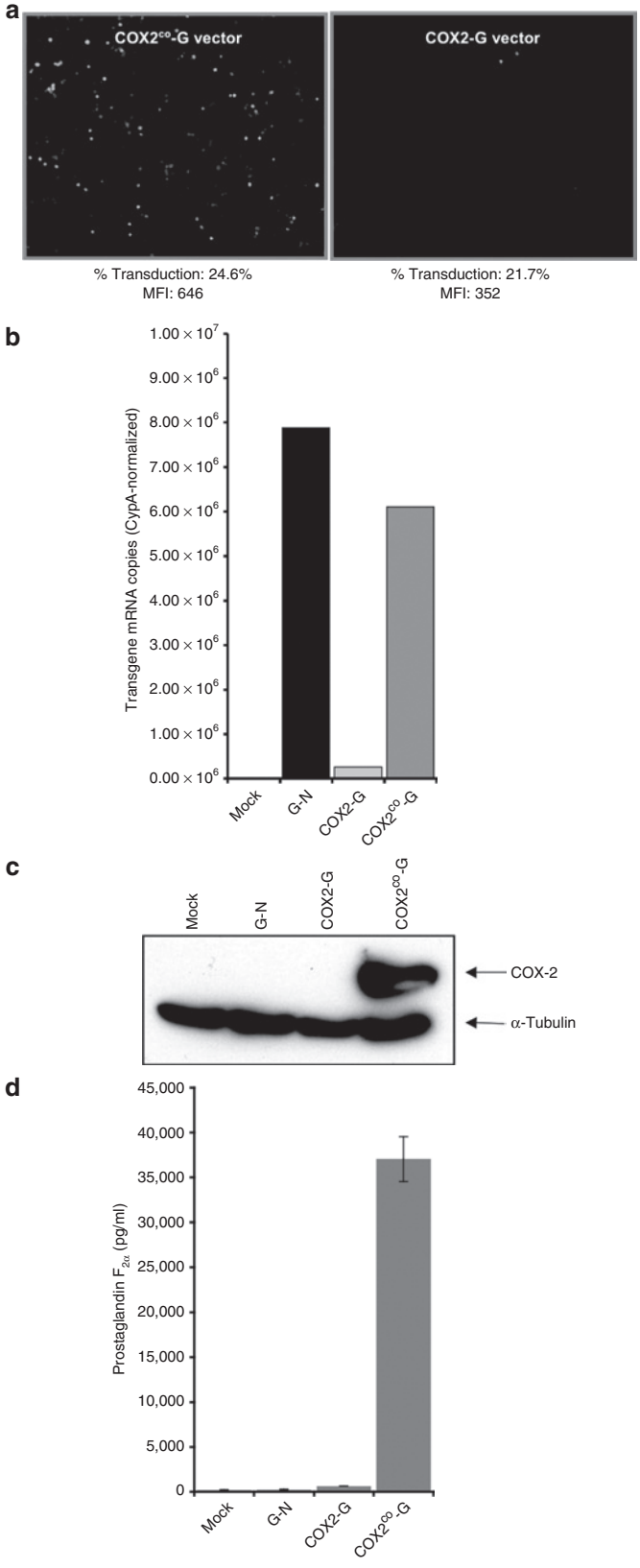

Completion of the pathway

Although COX enzymes are considered rate-limiting in PG pathways, synthesis of individual PGs requires specific downstream synthases,[4] so we also constructed a lentiviral vector encoding human PGF synthase [PGFS-G, **Figure 1b(iii)**], which was readily expressed from the native cDNA (**Figure 3a**). Finally, to attempt to establish a complete $PGF_{2\alpha}$ pathway, we generated a human FPR-encoding FIV vector. Like COX-2, the FPR coding region[25] displays an AU-skewed message (**Supplementary Figure S2b**). Interestingly, this composition is opposite to the GC-rich, human-optimal coding composition of the PGE_2 receptor (**Supplementary Figure S2b**). These dramatically different codon usages for two different human PG receptors suggest quite different signaling pathway-specific cellular strategies for RNA-level regulation. Based on this analysis, we synthesized a codon-optimized FPR allele (FPR^{co}) similar to the COX-2 vector; an N-terminal HA-epitope tag was also added [**Figure 1b(iv)**]. Functional integrity of HA-tagged FPR^{co} for signaling was verified with a luciferase reporter assay (**Supplementary Figure S4**).

$COX\text{-}2^{co}$ expression alone resulted in substantial PG production, with $PGF_{2\alpha}$ production exceeding PGD_2 and PGE_2 (**Figure 3b** and data not shown). By itself, PGFS expression had no effect on production of any PG in cultured cells, which is consistent with the known rate-limiting property of COX-2 in this pathway, but coexpression with $COX\text{-}2^{co}$ increased secreted $PGF_{2\alpha}$ selectively, as did FPR^{co} coexpression (**Figure 3b**). These results establish the ability to engineer a *de novo*, constitutive COX-2-based PG

Figure 2 Effects of COX-2 cDNA sequence optimization on mRNA levels, COX-2 protein levels, and same mRNA reporter expression. (**a**) *COX-2co* augments expression. 293T cells transduced with lentiviral vectors having either the *COX-2* or the *COX-2co* cDNA; in each vector, the cDNA is co-translated with green fluorescent protein (GFP) from within a single transcription unit [vector structures shown in **Figure 1b(i,ii)**]. This bicistronic single mRNA arrangement afforded by the internal ribosome entry site (IRES) allows GFP to function as the test gene. Fluorescence-activated cell sorting analysis showed that, as predicted, percent transduction was roughly equivalent (24.6% versus 21.7%). However, mean fluorescence intensity (MFI) was much lower with the native cDNA (352 for the COX2-G vector versus 646 for COX2co-G vector), corresponding to much less visible fluorescence detected microscopically. (**b**) mRNA measurements by real-time PCR. Total RNA from transduced 293T cells were analyzed by real-time quantitative reverse transcriptase–PCR for the COX-2-IRES-GFP and COX-2co-IRES-GFP mRNAs using GFP-specific primers. Copies were normalized for cyclophilin-A mRNA as previously described.[41] In equivalently transduced cells, mRNA levels were consistently more than tenfold higher with COX-2co. See **Supplementary Figure 3** for northern blotting. (**c**) COX-2 protein levels. Protein samples (50 µg) from transduced 293T cells were immunoblotted with antibody to human COX-2 (top row) or α-tubulin (bottom row). (**d**) Effect of sequence optimization on prostaglandin $F_{2\alpha}$ production. $PGF_{2\alpha}$ levels were determined in supernatants from 293T cells transduced at equivalent multiplicity of infection with the different lentiviral vectors.

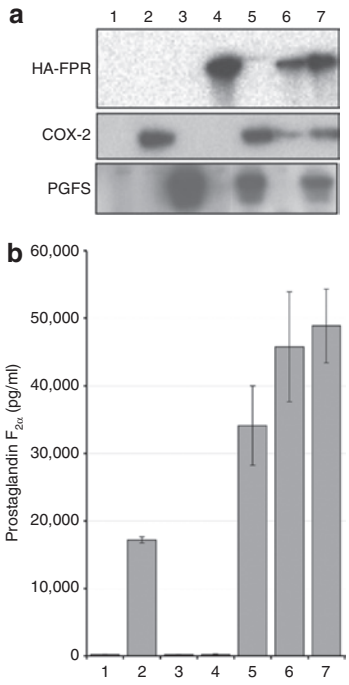

Figure 3 Expression of COX-2-based prostaglandin pathway components results in prostaglandin $F_{2\alpha}$ production. (**a**) Immunoblotting of 293T cell lysate for COX-2, PGFS, or FPR confirms expression. (**b**) PG production. $PGF_{2\alpha}$ production was assayed by enzyme immunoassay in media from **a**. COX-2 was necessary and sufficient to drive PG production in 293T cells, and addition of PGFS or FPR expression increased production. Error bars: standard deviations of triplicate samples. Data are representative of three separate experiments. 1, mock; 2, $COX2^{co}$-G; 3, PGFS-G; 4, FPR^{co}-G; 5, $COX2^{co}$-G + PGFS-G; 6, $COX2^{co}$-G + FPR^{co}-G; 7, $COX2^{co}$-G + PGFS-G + FPR^{co}-G.

biosynthesis and response pathway using integrated sequence-adjusted transgenes.

COX-2 pathway gene therapy produces sustained IOP reduction *in vivo*

For preclinical glaucoma studies, the cat eye AC is a good animal model for testing IOP-reducing therapeutics because of the feline eye's well-developed aqueous humor outflow pathway and human-comparable size (these are limiting features in mice and rats, where the lens dominates the AC and the TM is rudimentary). Although differences are discernible—Schlemm's canal in primates is replaced by an aqueous plexus in felines, and the AC is deeper in felines, leading to a wider iridocorneal angle—the basic process and control of aqueous outflow are quite similar.[26–29] The additional advantage of the much greater availability of these animals compared to nonhuman primates previously led to development of the cat model for glaucoma pharmaceutical testing[3] and subsequently as a glaucoma gene therapy vector-testing model.[13,16,17] No realistic actual disease model for POAG exists. Surgical or laser injuries to the full circumference of the TM can raise IOP. However, these approaches do not recapitulate the subtle outflow resistance problem in POAG and the gross injury destroys the therapeutic target, the TM. In addition, normotensive eyes are preferred for preclinical studies of candidate IOP-reducing POAG therapeutics because responses are predictive of efficacy in human glaucoma.[3] Thus, successful small molecule therapies appear to utilize mechanisms that are also present in the normal outflow pathway.

We previously demonstrated long-term lentiviral vector–mediated marker gene expression in both human and feline TM,[13,15–17] and persistent high-level GFP expression has now been established in the domestic cat TM for over 2 years.[17] Here, we used this animal model to test the influence of lentiviral vector delivery of COX-2, PGFS, FPR, or combinations of these genes on IOP *in vivo*.

Each eye of 15 specific pathogen-free domestic cats was administered a single transcorneal injection containing 10^7 transducing units of a given FIV vector in a 200 µl total volume after withdrawal of an equal volume of aqueous humor. Right eyes received one of the following combinations of vectors (three animals per group): group 1: $COX2^{co}$-G alone; group 2: $COX2^{co}$-G and PGFS-G; group 3: $COX2^{co}$-G, PGFS-G, and FPR^{co}-G; group 4: $COX2^{co}$-G and FPR^{co}-G, or group 5: FPR^{co}-G alone. Left eyes received the same dose of control FIV vector G-N. This intra-animal paired eye control design was used to control for interanimal variation and for potential nonspecific effects of FIV vector particle injection or intraocular foreign protein synthesis *per se*. Results of all 30 eyes are reported here in an intention-to-treat style analysis (no eyes were discarded from the study analysis at any point). The only attrition from the study was one animal in group 1 that died from an anesthesia accident at 3 months, such that IOP data from these two eyes are missing for the final 2 months.

Vectors were well tolerated, acutely and long-term. In addition to IOP measurements, clinical examinations and slit lamp microscopy were conducted to detect signs of inflammation or other adverse effects. One week after injection, three animals (two in group 3 and one in group 2) experienced mild-to-moderate conjunctival hyperemia associated with mild cells in the AC. This resolved after short duration anti-inflammatory treatment (ketoprofen administered for 5 days) and did not recur throughout the 5-month study. Thereafter, clinical signs of inflammation were absent, which was eventually corroborated by histopathological examination as described below.

Significant, sustained IOP reductions were achieved by the PG pathway vectors, with the combination of the $COX\text{-}2^{co}$ and FPR^{co} vectors producing the largest decrease (**Figure 4a,b**, $COX\text{-}2^{co}$ + PGFS + FPR^{co} treatment group: mean sustained IOP decrease = 4.73 mm Hg, 39% reduction, $P = 0.003$; $COX\text{-}2^{co}$ + FPR^{co} treatment group: mean sustained IOP decrease = 5.40 mm Hg, 35% reduction, $P = 0.03$). By way of comparison, $PGF_{2\alpha}$ analogue treatment (latanoprost) produces ~25% fall in IOP in human open-angle glaucoma patients, with a range of 22–39% reported in various studies.[30,31] Combining both experimental groups (*i.e.*, cats receiving at least $COX\text{-}2^{co}$ and FPR^{co}, $n = 6$) demonstrated a mean sustained IOP decrease of 5.07 mm Hg (32% reduction, $P = 0.0001$). Of the 12 eyes in this combined group, directly comparing the triplicate means from all individual IOP measurements in the six left eyes versus six right eyes yields a P value <10–18 ($n = 17$ triplicate measurements per eye over 5 months, done at one- to two-week intervals). The maximum effect at study termination at 150 days after injection was observed in an animal in the $COX\text{-}2^{co}$ + FPR^{co} treatment group, which demonstrated an IOP decrease of 7.50 mm Hg (42% reduction, right eye = 10.17 mm Hg,

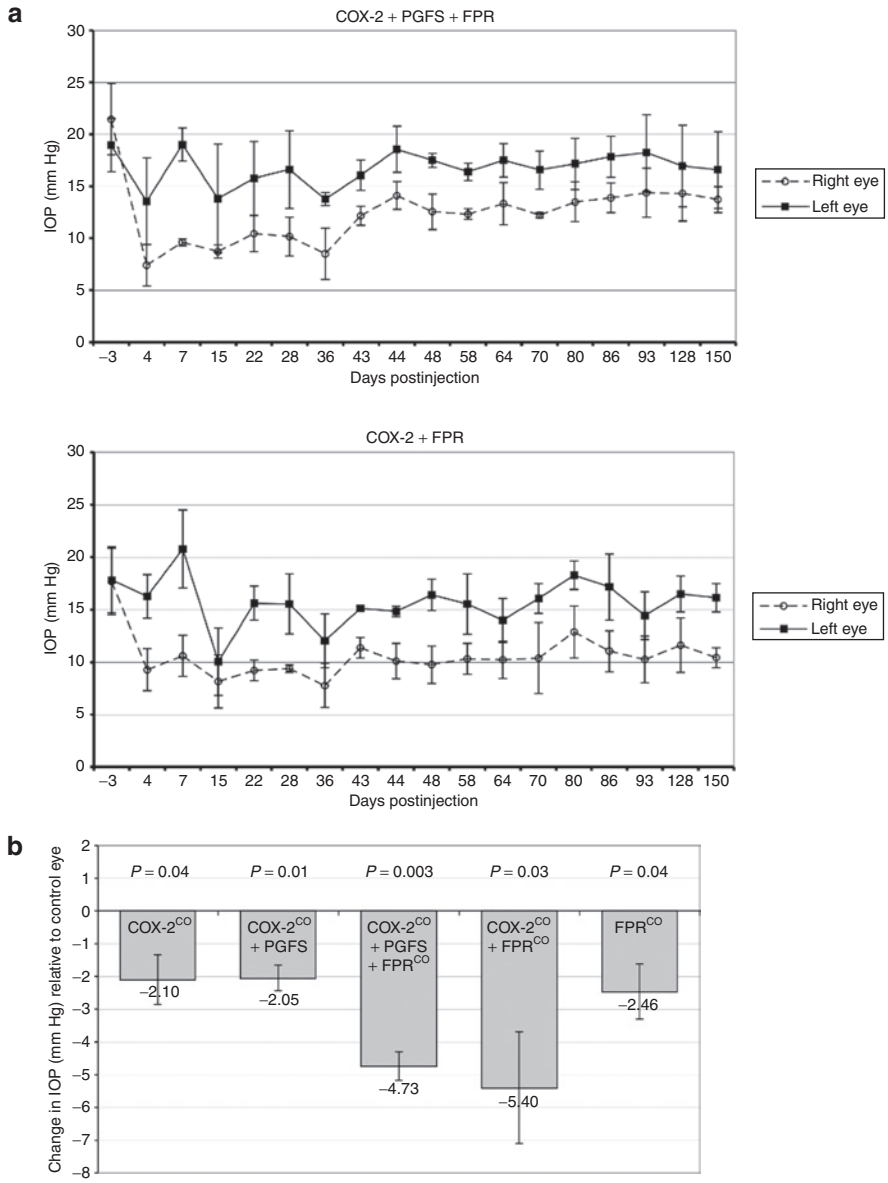

Figure 4 Effects of prostaglandin pathway lentiviral vectors on IOP in domestic cats. (**a**) Five-month IOP data from the two experimental groups (COX-2^{co} + PGFS + FPR^{co} and COX-2^{co} + FPR^{co}) with the largest IOP-reduction effect throughout the course of the study. Each right eye received a prostaglandin pathway vector (dashed lines) and was compared at each time point to its paired intra-animal control left eye, which received the control vector (solid lines). Each point is an average of the IOPs of the three animals in each experimental group at the given time after injection. Error bars represent the standard deviation of the mean IOP of the three animals. (**b**) Mean IOP differences (right eyes relative to control left eyes) over the course of study for each treatment group. Groups treated with at least COX-2^{co} and FPR^{co} demonstrated the greatest average IOP reductions relative to paired control left eyes. *P* values for two-tailed, paired *t*-tests comparing experimental right to control left eyes of each group are shown. Error bars represent the standard deviation of the mean sustained IOP difference of three animals. IOP, intraocular pressure.

left eye = 17.67 mm Hg). Because the COX-2^{co} + FPR^{co} treatment group demonstrated the largest average sustained IOP reduction, it appears that PGFS is dispensable in this system, suggesting that, as has been well described in other cell types and was evident in the tissue culture experiments, COX-2 is rate-limiting. In addition, capacity for a complete pathway, from biosynthesis to response, must be transferred to obtain substantial sustained IOP reduction. Interestingly, animals treated without the receptor, *i.e.*, with COX-2^{co} or COX-2^{co} + PGFS vectors, demonstrated an *initial* substantial decrease in IOP relative to control eyes (mean = 6.73 mm Hg), but this degree of reduction was not sustained for the past 2 weeks (**Supplementary Figure S5**). In the COX-2^{co} treatment group, the mean sustained IOP decrease over 5 months was 2.10 mm Hg (15% reduction, $P = 0.04$). Overall, the data suggest that the best sustained IOP effect requires introducing a complete ectopically expressed PG synthesis and response pathway.

Fluorophotometry indicates no reduction in aqueous humor flow

The reduction in IOP that we measured could be caused by either an increase in outflow facility or a reduction in aqueous humor flow, and the latter would suggest that the gene therapy suppressed

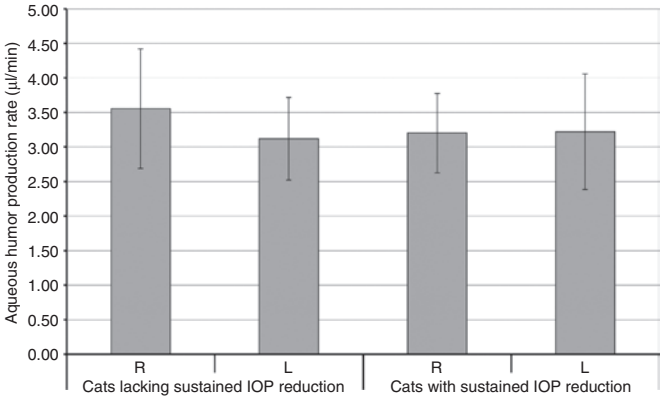

Figure 5 Aqueous humor flow rates in animals with and without sustained reduction of IOP. Treated eyes that maintained a large decrease in IOP (*i.e.*, all animals treated with at least COX-2^{co} and FPR^{co}, $n = 6$) had flow rates that were not significantly different from flow rates in control left eyes (mean change in flow rate = 0.02 ± 1.01 µl/min, *i.e.*, <1%, $P > 0.9$). Aqueous humor flow rate would have to have been reduced by 48% to have reduced IOP by the 5.07 mm Hg (32%) observed in treated eyes with sustained IOP reduction. By using the fluorophotometry method, we had an 80% probability ($\beta = 0.2$) of finding an actual reduction of at least 22% in flow rate, if flow had been suppressed by this much. The reduction in pressure could not be explained by an undetected difference in flow this small. Cats lacking sustained IOP reduction: all subjects in groups 1, 2, and 5. Cats with sustained IOP reduction: all subjects in groups 3 and 4. L, left; R, right. Bars represent mean flow rate of six or more eyes. Error bars represent 95% confidence intervals. IOP, intraocular pressure.

fluid production by the ciliary body. To distinguish between these two possible causes, we measured the aqueous humor flow rate in each eye by using fluorescein clearance measured by scanning fluorophotometry.[32] This technique is preferable to tonography, which is not standardized for use in the cat and which has low accuracy even in humans,[27,33] and in our hands, tonographic data were too noisy to be interpreted with statistical significance (data not shown). With scanning fluorophotometry, we found that aqueous humor flow rate was not significantly different between eyes with decreased IOP and paired control eyes (**Figure 5**, $P > 0.9$). Instead, as we hypothesized from the actions of PG analogues in the AC, we conclude that the IOP-lowering effect is caused by a change in outflow resistance.

Lentiviral vector transgene expression extends to both anterior and posterior chambers

The study was terminated by euthanasia at 5 months after vector injection, and all eyes were enucleated and studied with flat mount fluorescence microscopy, histology, and immunofluorescence. Transgene expression was visualized in all injected eyes but was absent as expected in uninjected control eyes (**Figure 6a**). An interesting and unexpected result was that transgene expression was detected not only in TM as we have seen previously in this model,[13] but also in the ciliary body NPE (**Figure 6b**). We believe that this contrast with our previous study is likely due to the fourfold larger vector bolus volume injected in the present study (200 versus 50 µl), which likely produced turbulence sufficient to distribute vector to both posterior and anterior chambers of the anterior segment. Postmortem histopathological examination of all eyes was also consistent with the lack of clinically evident inflammation determined by slit lamp observations during life. PG pathway vector–transduced eyes, control vector transduced eyes, and untransduced eyes were indistinguishable histopathologically. None showed inflammatory infiltrates or any changes in TM integrity, morphology, or cellularity (**Supplementary Figure S6**).

DISCUSSION

This study demonstrates that a therapeutic PG biosynthesis and response pathway can be engineered *in vivo*. It also provides the first effective transgene system for glaucoma gene therapy. These results have interest for basic research into biological roles of COX-2 and for their practical application to the specific disease problem of open-angle glaucoma. In the course of developing effective expression systems, we found that a native COX-2 coding region cDNA is poorly suited to ectopic expression. The AU-rich and codon-skewed base composition of the native cDNA message confers an expression block distinct from that known to result from 3′-UTR elements. In some tissues, this property may contribute to rapid clearance of COX-2 when this is a preferred physiological strategy. In those tissues in which COX-2 is constitutively expressed at substantial levels, *e.g.*, the ciliary body NPE, unknown mechanisms must act to counteract the intrinsic instability of the mRNA. Its base composition resembles that of Rev-dependent HIV mRNAs; in this regard, it has also recently been shown that the COX-2 mRNA, like Rev-dependent mRNAs, depends on the CRM1 nuclear export receptor pathway.[34] It will be of interest to investigate further how COX-2 mRNA is regulated at the level of nuclear processing and export because deciphering these mechanisms could contribute to better understanding of the role of COX-2 in health and disease, inside and outside the eye.

The combination of lentiviral vectors and codon-optimized transgene cassettes enabled stable ectopic expression in the eye. Gene expression occurred predominantly in TM as expected from prior studies, but an interesting result was the achievement of some expression in the posterior chamber of the anterior segment, in the NPE. Thus, the expanded targeting enabled us to access the region of the eye in which COX-2 expression is ablated in glaucoma. The IOP-reducing efficacy of the gene therapy would be compatible with a model where the disappearance of COX-2 from the NPE in glaucoma, which is striking for its completeness and disease subtype-specificity (POAG and steroid-induced glaucoma),[6] has pathogenic significance. IOP elevation alone clearly does not ablate COX-2 expression because eyes from patients with angle-closure and congenital forms of glaucoma display normal COX-2 expression despite chronic IOP elevation.[6] However, further studies are needed to establish the true causal direction of the association discovered by Maihöfner *et al*. We also emphasize that, the detectable NPE transduction notwithstanding, the *in vivo* and postmortem expression monitoring both suggest that the great majority of transduction occurred in TM, which would be predicted to lead to predominantly *local* PG production and effects. This focal targeting is advantageous because it prevents exposure to high PG levels throughout the AC, where they are not needed. Consistent with this interpretation, we found that differences between baseline and postinjection $PGF_{2\alpha}$ and PGE_2 levels could not be reliably determined in bulk aqueous humor because they were below the

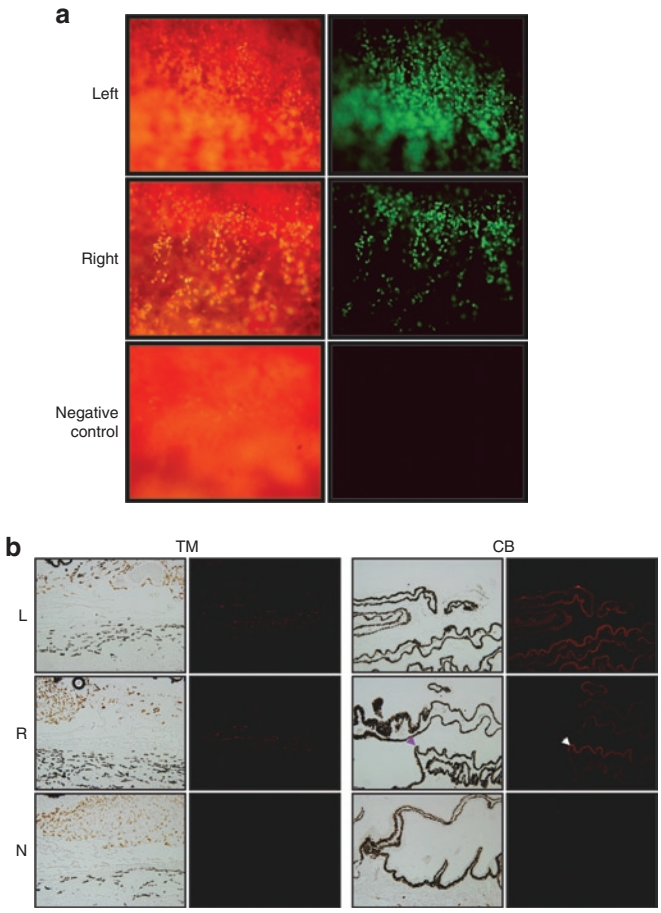

Figure 6 Transgene expression in trabecular meshwork (TM). (**a**) Direct assessment of GPF fluorescence in flat-mounted TM from freshly enucleated eye of cat treated 5 months earlier with COX2^{co}-G + FPR^{co}-G vector combination was imaged and photographed under white light (left panels) and UV light (right panels). Abundant GFP expression is evident. (**b**) Immunofluorescence analyses of eye tissues. Right eyes were transduced 5 months earlier with COX2^{co}-G and PGFS-G vectors; all vector groups showed similar staining. GFP was detected repeatedly in both TM tissue (left panels) and in the nonpigmented epithelium (arrow) of the ciliary body (right panels). Rabbit anti-GFP and secondary goat anti-rabbit were used. CB, ciliary body; L, left eye; N, negative control (uninjected) cat eye; R, right eye; TM, trabecular meshwork.

limit of EIA detection (data not shown). These results corroborate the findings of a human study using the same commercial EIA, where aqueous $PGF_{2\alpha}$ was not detectable in any of the 60 subjects and PGE_2 was barely detectable in less than half.[35]

Although COX-2 expression alone had some IOP-reducing effects, the maximal sustained effect resulted from transducing both COX-2^{co} and FPR^{co}. This result is in accord with the current concept that drugs such as latanoprost probably act by stimulating the endogenous FPR in the outflow pathway. The 35% IOP reduction we observed compares favorably with such topical PG analogue therapy, which produces ~25% reduction in IOP in humans, but which requires daily readministration.[30] Our data would be consistent with a model in which PG production and FPR activation lead to remodeling of the outflow tract to reduce outflow resistance, perhaps by upregulation of factors such as matrix metalloproteinases. Our results suggest that PGFS coexpression does not enhance IOP reduction and this is consistent with COX-2 being rate-limiting. It is possible, however, that because PGFS is transduced using a separate vector, not enough cells are co-transduced with both genes to see synergy. This suggests an opportunity that can be explored in the future with a dual-gene vector. Future studies can also explore the effects of PG analogues on transduced eyes. Increased expression and availability of PG receptors in a transduced outflow tract could augment IOP-reducing effects. The cat eye is of particular interest as $PGF_{2\alpha}$ isopropyl ester results in impressive IOP reduction whereas the modification of this analogue to latanoprost abrogates the effect.[3] Given the increased receptor specificity of latanoprost, feline eyes transduced with human FPR could yield additional insights distinguishing human and feline FPR function.

The source of arachidonic acid substrate for COX-2 may be the transduced TM cells themselves. For example, Luna and colleagues reported that porcine TM cells subjected to cyclic mechanical stress release ATP that activates purinergic receptors, in turn leading to mobilization of arachidonic acid from the plasma membrane.[36] Whatever the source of initial substrate, the enzyme is likely to be rate-limiting in PG production.

Although we can conclude securely that the mechanism of IOP reduction is not the result of decreased aqueous production, we cannot distinguish between facility enhancement at the pressure-dependent conventional outflow pathway versus the uveoscleral outflow pathway. In addition, the proportion of aqueous humor that exits via the uveoscleral route varies significantly between species, and it is thus difficult to estimate what fraction normally exits by this route in the cat eye and to what extent this gene therapy is affecting each route. Previous studies suggest that the uveoscleral pathway is only responsible for about 3% of the total feline aqueous outflow, *i.e.*, much lower compared to canines and primates.[37] Given that the TM is the predominant transduction site, we suspect greater effects occur at the conventional outflow pathway. Potential paracrine-like effects of transduced TM on more posterior tissues are possible. Additionally, some studies have demonstrated that PG analogues induce increased facility at the conventional outflow tract. Bahler *et. al.* removed the variable of the uveoscleral tract in the perfusion AC system to demonstrate that PG analogues increase conventional outflow facility.[38] The extent of conventional outflow pathway involvement in IOP reduction induced by PG agonists may thus be underestimated.

Human gene therapy remains challenged in the real-world clinical setting by the problem of scale, *i.e.*, the practical difficulty of achieving enough transgene delivery to be effective. The field has, in part, approached the problem by prioritizing a few proof-of-concept diseases, *e.g.*, those in which gene-corrected cells have a marked proliferative advantage (X-linked SCID, ADA) or in which very little transgene expression may be predicted to have a systemic effect. Here, we focus on a small, physiologically critical target, the TM, where fewer than a half million cells need transgene introduction. The cat AC is actually slightly larger than the human AC, so that our animal model is quantitatively realistic for projecting clinical practicality. Our results also provide a conceptual and experimental platform for pursuing further variations of the engineered PG biosynthesis and response pathway theme. Although other PGs have effects on IOP (*e.g.*, PGE_2), it will be of

interest to determine in future studies whether gene therapy that transduces alternative downstream PG synthases or PG receptors into the AC can reduce IOP. For example, the PG EP receptor subtypes 1–4 deserve attention because in the cat, the EP_1 receptor seems to account for some of the IOP-reducing effects of $PGF_{2\alpha}$,[39] and evidence for expression of these receptors has been found in anterior segment tissues from a variety of species, including humans.[40] Lentiviral vectors are also capable of effecting highly effective RNA interference,[41] which could be directed at mRNAs for PG pathway components or other molecules relevant to IOP pathophysiology.

MATERIALS AND METHODS

FIV vectors. The GFP allele in all constructs is the enhanced (eGFP) version. To construct transfer vector pCOX2-G, a human COX-2 cDNA (a gift of Timothy Hla, University of Connecticut) was inserted as a Klenow polymerase-blunted *Not*I-*Xba*I fragment into the Klenow-blunted *Age*I-*Eco*RI backbone of pG-N [**Figure 1b(v)**]. pG-N has also been referred to by its longer name pGiNWF in some prior publications.[15,16,41,42] Next, the IRES-GFP cassette of pIRES2eGFP was released by *Eco*RI-*Mfe*I digestion and blunt end-ligated into the *Eco*RI site just downstream of the COX-2 cDNA insert. For pCOX2^{co}-G and pFPR^{co}-G, codon-optimized human COX-2 and HA-tagged FPR cDNAs with useful flanking restriction sites were designed. Full synthetic gene sequences are available on request. G-C content was optimized, and secondary structure and repetitive codons were considered in a computerized algorithm, and synthetic cDNAs were synthesized by GenScript (Scotch Plains, NJ). Final genes were verified by Sanger sequencing. Optimization introduced 382 and 274 nt changes into the 1815 nt COX-2 and 1107 nt FPR sequences, respectively. Flanking BamHI sites were included in the synthesis to enable insertion into the *Bam*HI backbone of pCOX2-G, thus replacing the wild-type allele with the synthetic codon-optimized allele. For pPGFS-G, the human PGFS cDNA from hPGFS-cDNA pUC8 (ref. 43) (a gift of Kikuko Watanabe, University of East Asia, Japan) was removed by EcoRI-SalI digestion and blunt end-ligated into the BamHI backbone of pCOX2-G.

PGF2α EIA. 293T cells in 6 well plates were transduced with COX2^{co}-G, PGFS-G, or FPR^{co}-G lentiviral vectors as previously described;[44] 36 hours later, medium was filtered (0.2 mmol/l) and assayed with a $PGF_{2\alpha}$ enzyme immunoassay kit (Cayman Chemical) following the manufacturer's instructions. These experiments were also repeated by direct transfection of 2 μg pCOX2^{co}-G, pPGFS-G, or pFPR^{co}-G using calcium phosphate coprecipitation.

Northern blotting. Cellular RNAs were harvested with 1 ml Trizol at 36 hours, extracted with chloroform followed by isopropanol, and centrifuged to pellet nucleic acid. Nucleic acid was treated with DNase, followed by extraction with equal volume of phenol:chloroform:isoamyl alcohol (125:24:1). RNA was precipitated with 1/10 volume 3 mol/l sodium acetate and 2.5 volumes 100% ethanol. Total cellular RNA was separated by gel electrophoresis (1.2% agarose, 3.75% formaldehyde, 1× MOPS) and transferred to a nylon membrane. A β-actin antisense oligonucleotide probe (5′-AGGGGCCGGACTCGTCATACT-3′) was 5′-end labeled using T4 polynucleotide kinase (Promega, Madison, WI) and [γ-^{32}P]ATP, with incubation at 37 °C for 30 minutes followed by heat inactivation at 70 °C for 10 minutes. Labeled probe was purified using a quick spin column and hybridized overnight at 42 °C, washed, and exposed to X-ray film at −80 °C for 5 days. For the GFP probe, 25 ng of GFP antisense oligonucleotide (5′-CCGGGCCCGCGGTACCGTCGACTGCAGAATTCGAAG CT-3′) was randomly labeled using 50 mCi α-dCTP in the presence of 20 mmol/l dATP, dTTP, and dGTP and Klenow fragment at 37 °C for 1 hour and then heat-inactivated at 65 °C for 10 minutes. Random-labeled probe was purified using a quick spin column followed by hybridization with the RNA-containing nylon membrane overnight, followed by washing and exposure to x-ray film for 5 hours to 3 days at −80 °C.

Real-time quantitative PCR. Total RNA was harvested using the Qiagen Rneasy Mini-kit (Qiagen, Germantown, MD). Two microgram of mRNA was converted to cDNA using the Superscript III First Strand Synthesis System for reverse transcriptase–PCR with oligo(dT) primers (Invitrogen, Carlsbad, CA). Amplifications were done in a Roche LightCycler with Roche LCDA software using the Roche FastStart DNA Master SYBR Green Kit I (cat. no. 03 003 230 001). Cyclophilin-A primers were 5′–TTCATCTGCACTGCCAAGAC–3′ and 5′–TGGTCTTGCCATTCCTGGAC–3′, which were used for sample normalization. Primer sequences for eGFP were 5′–AGAACGG CATCAAGGTGAAC–3′ and 5′–TGCTCAGGTAGTGGTTGTCG–3′. LightCycler programs included an initial denaturation step at 94 °C for 10 minutes and a melting step after amplification (40–94 °C, temperature transition rate = 0.20 °C/seconds). PCR conditions were 94 °C for 10 seconds, 62 °C for 30 seconds, 72 °C for 13 seconds, ×50 cycles with temperature transition rate = 5 °C/second.

FPR reporter assay. The assay is based on that of Liang *et al.*[45] We amplified the Nur77 promoter from human genomic DNA using primers 5′–AAGCTAGCGGCTTGGGAAGGTGTAAAGGC–3′ and 5′–AA ACTCGAGGTTTCCGTAGCCTCCGCCAC–3′ and inserted the amplicon into the multiple cloning site of pGL3-Basic (Promega) to yield a construct with Nur77 promoter-dependent firefly luciferase expression (pNur77-luc). An FPR expressing cell line (293T-FPR) was generated by transduction with FPR^{co}-G FIV vector, followed by fluorescence-activated cell sorting for GFP. 293T and 293T-FPR cells were then transfected with pNur77-Luc, with a *Renilla* luciferase expression plasmid co-transfected to control for transfection efficiency. Cell lysates were assayed with the Dual Luciferase Reporter Assay (Promega) and expressed as *Renilla*-adjusted firefly luciferase units.

Immunoblotting. Cells were lysed in Tris-buffered saline containing 1% Triton X-100 and 1% NP-40, plus a protease inhibitor cocktail (Complete-mini; Boehringer, Ridgefield, CT). Lysates were centrifuged to remove chromatin and debris, and proteins were resolved in SDS-10% polyacrylamide gels and transferred to Immobilon P membranes (Millipore, Billerica, MA). Blocked membranes were incubated overnight at 4 °C or for 2 hours at room temperature with anti-COX-2 mAb (Cayman Chemical, 160112), rat anti-HA (Roche), or rabbit anti-hPGFS (a gift from Kikuko Watanabe). After washing, membranes were incubated with the appropriate horseradish peroxidase–tagged secondary antibody. Conjugated antibodies were detected by ECL (Amersham Pharmacia Biotech, Piscataway, NJ).

Vector production and injection. FIV vectors were produced, titered and tested for reverse transcriptase activity as previously described.[42,44] Specific pathogen-free domestic cats were purchased (Harlan, Indianapolis) and handled in accordance with Institutional Animal Care and Use Committee regulations. Ten- to twelve-week-old cats were anesthetized with 10 mg/kg intramuscular tiletamine HCl/zolazepam HCl (Telazol; Fort Dodge Laboratories, Fort Dodge, IA) injection, and ACs were injected transcorneally as previously described.[13] Each injection contained 10^7 TU of vector in 200 μl PBS, which was delivered to the AC as a replacement volume (200 ml of aqueous humor was withdrawn immediately prior to vector injection).

IOP measurements and slit lamp examinations. Prior to examinations, cats were anesthetized with 10 mg/kg intramuscular Telazol injection. Weekly examinations involved clinical assessment, slit lamp (Haag-Streit, Mason, OH) observation, and determination of IOP using a digital

pneumatonometer (Model 30 Classic; Medtronic, Fridley, MN). IOP was recorded as the average of 3 measurements over 5 minutes.

Scanning fluorophotometry. Aqueous humor flow was measured 3–4 months after injection of the vector. Briefly, 5–7 drops of 2% sodium fluorescein solution were topically instilled in each eye. Fluorescein concentrations in the AC and cornea were measured 8, 12, and 16 hours later by using a scanning ocular fluorophotometer.[32] This instrument employs a 488 nm argon laser to scan a measurement window in a horizontal plane through the anterior segment of the eye. A two-dimensional array is reconstructed of fluorescence, equivalent to fluorescein concentrations in a 4 log range (10^{-10} to 10^{-6}g/ml).[32] Fluorescence in the AC and cornea was selected from graphs of fluorescence with depth, and the mean fluorescein concentrations in the cornea and AC were determined. Aqueous humor flow rate was determined from the decrease in fluorescein concentrations between consecutive measurements:

$$\text{Flow} = \frac{-(\Delta C_c V_c + \Delta C_a V_a)}{\overline{C_a}\,dt} - 0.25\,\mu\text{l/min} \quad (1)$$

where V_c and V_a are the volumes of the cornea and AC, respectively, ΔC_c and ΔC_a are the changes in fluorescein concentration in the cornea and AC, respectively, on interval dt, and $\overline{C_a}$ is the average concentration of fluorescein in the AC during the interval.[46] The reduction by 0.25 µl/min in equation 1 accounts for a small amount of fluorescein that leaves the AC by diffusion directly into the iris and not through outflow pathways.[47]

Flat mount fluorescence imaging, immunofluorescence, immunohistochemistry, and histopathology. Enucleated eyes were dissected, and intact TM was imaged for GFP expression under a fluorescent microscope. Anterior segment tissues including cornea, TM, iris, and ciliary body were fixed in 4% paraformaldehyde, infiltrated with paraffin and cut in 6-µm sections. Tissue was deparaffinated and antigen retrieval was achieved by boiling in 0.05% citraconic anhydride (pH 7.4). Rabbit anti-GFP (Novus NB 600-303, 1:500) was used for primary antibody. Alexa Fluor 594 goat anti-rabbit IgG (Invitrogen A11037, 1:100) was used as secondary antibody. Specimens were examined and photographed by using a digital camera mounted on an Olympus BX60F5 light-field/fluorescence microscope. Hematoxylin and eosin–stained sections from all four AC quadrants of all eyes including control uninjected eyes were scored in random order by a masked observer for inflammation, overall morphology, fine trabecular structure, and cellularity.

Statistical methods. Mean sustained IOP in each eye was calculated as the average of 17 measurements of IOP through the 5 months of the study (each measurement being the average of three consecutive determinations over 5 minutes with a digital pneumatonometer as described above). The sustained IOP of each treatment group was the average of the IOP from all eyes in the group. Differences in mean sustained IOP between treated and control eyes were examined by using paired *t*-tests (two-tailed, $\alpha = 0.05$: Excel, Microsoft, Seattle, WA).

The aqueous humor flow reduction that would be sufficient to explain the decreased IOP without a change in outflow resistance was estimated by using the Goldmann equation:

$$\text{Flow} = C_{\text{fl}}(\text{IOP} - P_e) + F_{\text{us}} \quad (2)$$

where Flow is the flow rate of aqueous humor, C_{fl} is outflow facility, IOP is intraocular pressure, P_e is episcleral venous pressure, and F_{us} is uveoscleral flow. We assumed $C_{\text{fl}} = 0.24$ µl/min/mm Hg (measured in this experiment), $F_{\text{us}} = 0.80$ µl/min, and $P_e = 5$ mm Hg. The minimum detectable difference in aqueous humor flow rate determine by fluorophotometry was estimated by using a power calculation with $\beta = 0.20$ and $\alpha = 0.05$, and assuming a reference flow rate of 3.16 ± 0.85 µl/min (mean ± SD), that we measured in untreated control eyes.

SUPPLEMENTARY MATERIAL

Figure S1. Circulatory physiology of the anterior segment of the eye.
Figure S2. Sequence analyses of different mRNAs.
Figure S3. COX-2 gene expression in transfected cells.
Figure S4. FPR activity.
Figure S5. IOP over time for each animal group.
Figure S6. H&E histology of anterior chamber tissue.

ACKNOWLEDGMENTS

We thank Douglas H. Johnson, Pranay Khare, J. Douglas Cameron, Nils Loewen, Mary Peretz, Dyana Saenz, Wulin Teo, and Thomas Rinkoski for valuable help and discussions; Cherie Nau for assistance with fluorophotometry; Timothy Hla for a COX-2 complementary DNA (cDNA); Garrett Fitzgerald for a human FP receptor cDNA; Kikuko Watanabe for a PGFS cDNA and rabbit anti-PGFS antibody; and J. Douglas Cameron and Adele K. Fielding for reviewing the manuscript. Supported by NIH (National Institutes of Health) grant EY14411.

REFERENCES

1. Bahrami, H (2006). Causal inference in primary open angle glaucoma: specific discussion on intraocular pressure. *Ophthalmic Epidemiol* **13**: 283–289.
2. Schwartz, G (2006). *Adherence and persistence in glaucoma*. In: Grehn, F and Stamper, R (eds). Glaucoma. Springer: New York, pp. 91–105.
3. Stjernschantz, JW (2001). From PGF(2alpha)-isopropyl ester to latanoprost: a review of the development of xalatan: the Proctor Lecture. *Invest Ophthalmol Vis Sci* **42**: 1134–1145.
4. Smith, WL, DeWitt, DL and Garavito, RM (2000). Cyclooxygenases: structural, cellular, and molecular biology. *Annu Rev Biochem* **69**: 145–182.
5. Egan, KM, Lawson, JA, Fries, S, Koller, B, Rader, DJ, Smyth, EM *et al.* (2004). COX-2-derived prostacyclin confers atheroprotection on female mice. *Science* **306**: 1954–1957.
6. Maihöfner, C, Schlötzer-Schrehardt, U, Gühring, H, Zeilhofer, HU, Naumann, GO, Pahl, A *et al.* (2001). Expression of cyclooxygenase-1 and -2 in normal and glaucomatous human eyes. *Invest Ophthalmol Vis Sci* **42**: 2616–2624.
7. Funk, CD (2001). Prostaglandins and leukotrienes: advances in eicosanoid biology. *Science* **294**: 1871–1875.
8. Grosser, T, Fries, S and FitzGerald, GA (2006). Biological basis for the cardiovascular consequences of COX-2 inhibition: therapeutic challenges and opportunities. *J Clin Invest* **116**: 4–15.
9. Hinz, B, Rösch, S, Ramer, R, Tamm, ER and Brune, K (2005). Latanoprost induces matrix metalloproteinase-1 expression in human nonpigmented ciliary epithelial cells through a cyclooxygenase-2-dependent mechanism. *FASEB J* **19**: 1929–1931.
10. Rösch, S, Ramer, R, Brune, K and Hinz, B (2005). Prostaglandin E2 induces cyclooxygenase-2 expression in human non-pigmented ciliary epithelial cells through activation of p38 and p42/44 mitogen-activated protein kinases. *Biochem Biophys Res Commun* **338**: 1171–1178.
11. Hattenhauer, MG, Johnson, DH, Ing, HH, Herman, DC, Hodge, DO, Yawn, BP *et al.* (1998). The probability of blindness from open-angle glaucoma. *Ophthalmology* **105**: 2099–2104.
12. Borrás, T, Brandt, CR, Nickells, R and Ritch, R (2002). Gene therapy for glaucoma: treating a multifaceted, chronic disease. *Invest Ophthalmol Vis Sci* **43**: 2513–2518.
13. Loewen, N, Fautsch, MP, Teo, WL, Bahler, CK, Johnson, DH and Poeschla, EM (2004). Long-term, targeted genetic modification of the aqueous humor outflow tract coupled with noninvasive imaging of gene expression in vivo. *Invest Ophthalmol Vis Sci* **45**: 3091–3098.
14. Loewen, N and Poeschla, EM (2005). Lentiviral vectors. *Adv Biochem Eng Biotechnol* **99**: 169–191.
15. Loewen, N, Fautsch, MP, Peretz, M, Bahler, CK, Cameron, JD, Johnson, DH *et al.* (2001). Genetic modification of human trabecular meshwork with lentiviral vectors. *Hum Gene Ther* **12**: 2109–2119.
16. Loewen, N, Bahler, C, Teo, WL, Whitwam, T, Peretz, M, Xu, R *et al.* (2002). Preservation of aqueous outflow facility after second-generation FIV vector-mediated expression of marker genes in anterior segments of human eyes. *Invest Ophthalmol Vis Sci* **43**: 3686–3690.
17. Khare, PD, Loewen, N, Teo, W, Barraza, RA, Saenz, DT, Johnson, DH *et al.* (2008). Durable, safe, multi-gene lentiviral vector expression in feline trabecular meshwork. *Mol Ther* **16**: 97–106.
18. Barraza, RA and Poeschla, EM (2008). Human gene therapy vectors derived from feline lentiviruses. *Vet Immunol Immunopathol* **123**: 23–31.
19. Barraza, RA, Rasmussen, CA, Loewen, N, Cameron, JD, Gabelt, BT, Teo, WL *et al.* (2009). Prolonged transgene expression with lentiviral vectors in the aqueous humor outflow pathway of nonhuman primates. *Hum Gene Ther* **20**: 191–200.
20. Shaw, G and Kamen, R (1986). A conserved AU sequence from the 3′ untranslated region of GM-CSF mRNA mediates selective mRNA degradation. *Cell* **46**: 659–667.

21. Appleby, SB, Ristimäki, A, Neilson, K, Narko, K and Hla, T (1994). Structure of the human cyclo-oxygenase-2 gene. *Biochem J* **302 (Pt 3)**: 723–727.
22. Newton, R, Seybold, J, Liu, SF and Barnes, PJ (1997). Alternate COX-2 transcripts are differentially regulated: implications for post-transcriptional control. *Biochem Biophys Res Commun* **234**: 85–89.
23. Lu, S, Yu, G, Zhu, Y and Archer, MC (2005). Cyclooxygenase-2 overexpression in MCF-10F human breast epithelial cells inhibits proliferation, apoptosis and differentiation, and causes partial transformation. *Int J Cancer* **116**: 847–852.
24. Schwartz, S, Felber, BK and Pavlakis, GN (1992). Distinct RNA sequences in the gag region of human immunodeficiency virus type 1 decrease RNA stability and inhibit expression in the absence of Rev protein. *J Virol* **66**: 150–159.
25. Kunapuli, P, Lawson, JA, Rokach, J and FitzGerald, GA (1997). Functional characterization of the ocular prostaglandin f2alpha (PGF2alpha) receptor. Activation by the isoprostane, 12-iso-PGF2alpha. *J Biol Chem* **272**: 27147–27154.
26. Richardson, TM, Marks, MS, Ausprunk, DH and Miller, M (1985). A morphologic and morphometric analysis of the aqueous outflow system of the developing cat eye. *Exp Eye Res* **41**: 31–51.
27. Wang, YL, Toris, CB, Zhan, G and Yablonski, ME (1999). Effects of topical epinephrine on aqueous humor dynamics in the cat. *Exp Eye Res* **68**: 439–445.
28. Aubin, ML, Powell, CC, Gionfriddo, JR and Fails, AD (2003). Ultrasound biomicroscopy of the feline anterior segment. *Vet Ophthalmol* **6**: 15–17.
29. Tripathi, RC and Tripathi, BJ (1972). The mechanism of aqueous outflow in lower mammals. *Exp Eye Res* **14**: 73–79.
30. Dinslage, S, Hueber, A, Diestelhorst, M and Krieglstein, G (2004). The influence of latanoprost 0.005% on aqueous humor flow and outflow facility in glaucoma patients: a double-masked placebo-controlled clinical study. *Graefes Arch Clin Exp Ophthalmol* **242**: 654–660.
31. Perry, CM, McGavin, JK, Culy, CR and Ibbotson, T (2003). Latanoprost: an update of its use in glaucoma and ocular hypertension. *Drugs Aging* **20**: 597–630.
32. McLaren, JW and Brubaker, RF (1985). A two-dimensional scanning ocular fluorophotometer. *Invest Ophthalmol Vis Sci* **26**: 144–152.
33. Wheeler, NC, Lee, DA, Cheng, Q, Ross, WF and Hadjiaghai, L (1998). Reproducibility of intraocular pressure and outflow facility measured by pneumatic tonography and Schiotz tonography. *J Ocul Pharmacol Ther* **14**: 5–13.
34. Jang, BC, Muñoz-Najar, U, Paik, JH, Claffey, K, Yoshida, M and Hla, T (2003). Leptomycin B, an inhibitor of the nuclear export receptor CRM1, inhibits COX-2 expression. *J Biol Chem* **278**: 2773–2776.
35. Matsuo, T (2004). Prostaglandins F2alpha and E2 in aqueous humor of patients with cataract surgery. *J Ocul Pharmacol Ther* **20**: 101–106.
36. Luna, C, Li, G, Qiu, J, Challa, P, Epstein, DL and Gonzalez, P (2009). Extracellular release of ATP mediated by cyclic mechanical stress leads to mobilization of Arachidonic Acid in Trabecular Meshwork cells. *Invest Ophthalmol Vis Sci* (epub ahead of print).
37. Alm, A and Nilsson, SF (2009). Uveoscleral outflow--a review. *Exp Eye Res* **88**: 760–768.
38. Bahler, CK, Howell, KG, Hann, CR, Fautsch, MP and Johnson, DH (2008). Prostaglandins increase trabecular meshwork outflow facility in cultured human anterior segments. *Am J Ophthalmol* **145**: 114–119.
39. Bhattacherjee, P, Williams, BS and Paterson, CA (1999). Responses of intraocular pressure and the pupil of feline eyes to prostaglandin EP1 and FP receptor agonists. *Invest Ophthalmol Vis Sci* **40**: 3047–3053.
40. Schlötzer-Schrehardt, U, Zenkel, M and Nüsing, RM (2002). Expression and localization of FP and EP prostanoid receptor subtypes in human ocular tissues. *Invest Ophthalmol Vis Sci* **43**: 1475–1487.
41. Llano, M, Saenz, DT, Meehan, A, Wongthida, P, Peretz, M, Walker, WH *et al.* (2006). An essential role for LEDGF/p75 in HIV integration. *Science* **314**: 461–464.
42. Saenz, DT, Barraza, R, Loewen, N, Teo, W and Poeschla, E (2006). *Production and use of feline immunodeficiency virus (FIV)-based lentiviral vectors.* In: Rossi, J and Friedman, T (eds). Gene Transfer: A Cold Spring Harbor Laboratory Manual. Cold Spring Harbor Laboratory Press: Cold Spring Harbor, NY. pp. 57–74.
43. Suzuki-Yamamoto, T, Nishizawa, M, Fukui, M, Okuda-Ashitaka, E, Nakajima, T, Ito, S *et al.* (1999). cDNA cloning, expression and characterization of human prostaglandin F synthase. *FEBS Lett* **462**: 335–340.
44. Loewen, N, Barraza, R, Whitwam, T, Saenz, DT, Kemler, I and Poeschla, EM (2003). FIV Vectors. *Methods Mol Biol* **229**: 251–271.
45. Liang, Y, Li, C, Guzman, VM, Chang, WW, Evinger, AJ, Pablo, JV *et al.* (2004). Upregulation of orphan nuclear receptor Nur77 following PGF(2alpha), Bimatoprost, and Butaprost treatments. Essential role of a protein kinase C pathway involved in EP(2) receptor activated Nur77 gene transcription. *Br J Pharmacol* **142**: 737–748.
46. Brubaker, RF (1994). *Clinical evaluation of the circulation of aqueous humor.* In: Tarman, WJ and Jaeger, EA (eds). Duane's Clinical Ophthalmology, vol. **3**. J.B. Lippincott: Philadelphia, PA. pp 1–11.
47. Brubaker, RF (1998). *Clinical measurements of aqueous dynamics: implications for addressing glaucoma.* In: Civan, M (ed.). The Eye's Aqueous Humor. Academic Press: San Diego, CA. pp 233–284.
48. Poeschla, EM, Wong-Staal, F and Looney, DJ (1998). Efficient transduction of nondividing human cells by feline immunodeficiency virus lentiviral vectors. *Nat Med* **4**: 354–357.
49. Whitwam, T, Peretz, M and Poeschla, E (2001). Identification of a central DNA flap in feline immunodeficiency virus. *J Virol* **75**: 9407–9414.
50. Kemler, I, Azmi, I and Poeschla, EM (2004). The critical role of proximal gag sequences in feline immunodeficiency virus genome encapsidation. *Virology* **327**: 111–120.